Fig S1

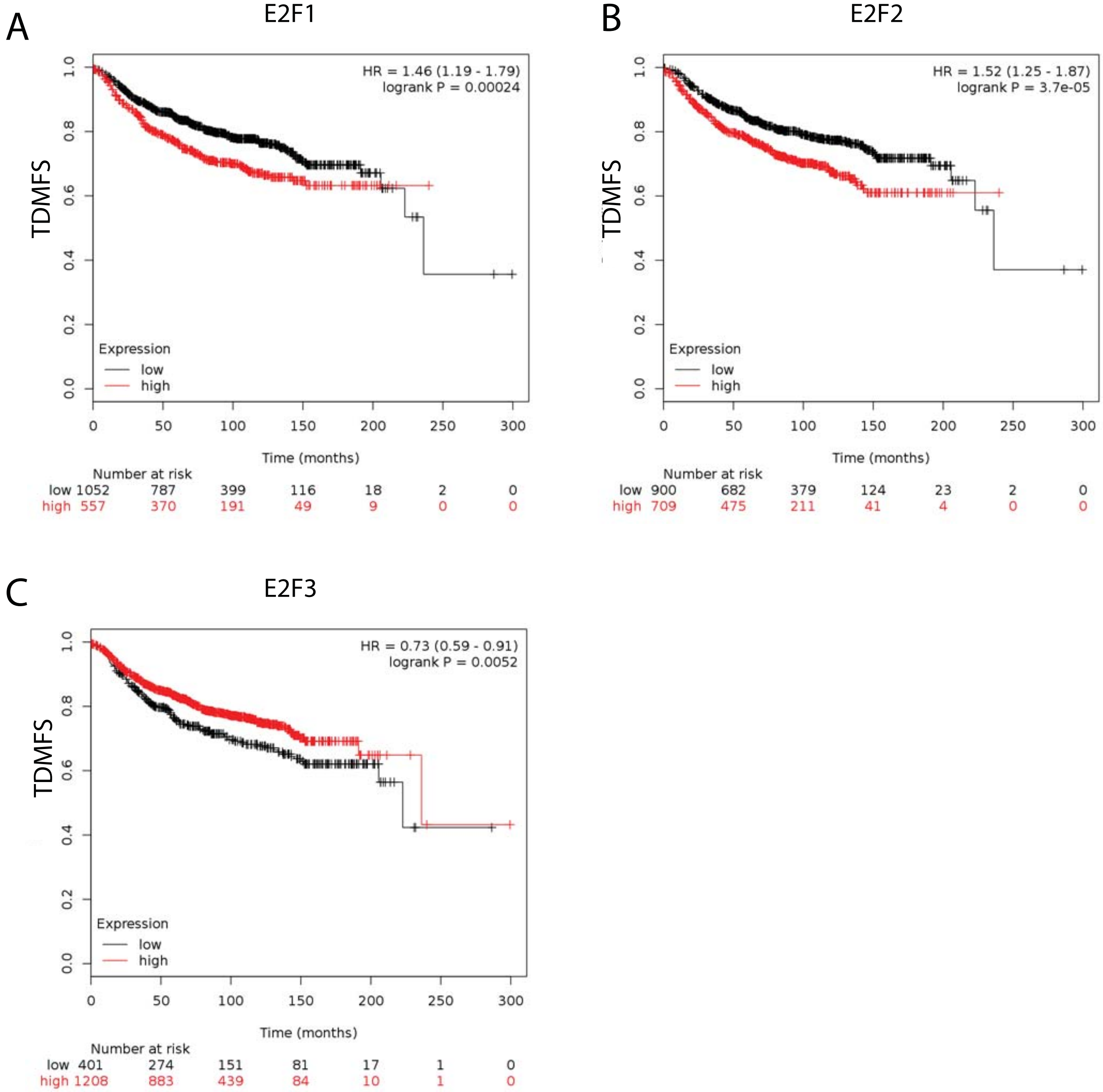
A
E2F1
HR = 1.46 (1.19 - 1.79)
logrank P = 0.00024
TDMFS
Expression
low
high
Time (months)
Number at risk
low 1052 787 399 116 18 2 0
high 557 370 191 49 9 0 0
B
E2F2
HR = 1.52 (1.25 - 1.87)
logrank P = 3.7e-05
TDMFS
Expression
low
high
Time (months)
Number at risk
low 900 682 379 124 23 2 0
high 709 475 211 41 4 0 0
C
E2F3
HR = 0.73 (0.59 - 0.91)
logrank P = 0.0052
TDMFS
Expression
low
high
Time (months)
Number at risk
low 401 274 151 81 17 1 0
high 1208 883 439 84 10 1 0

Fig S2

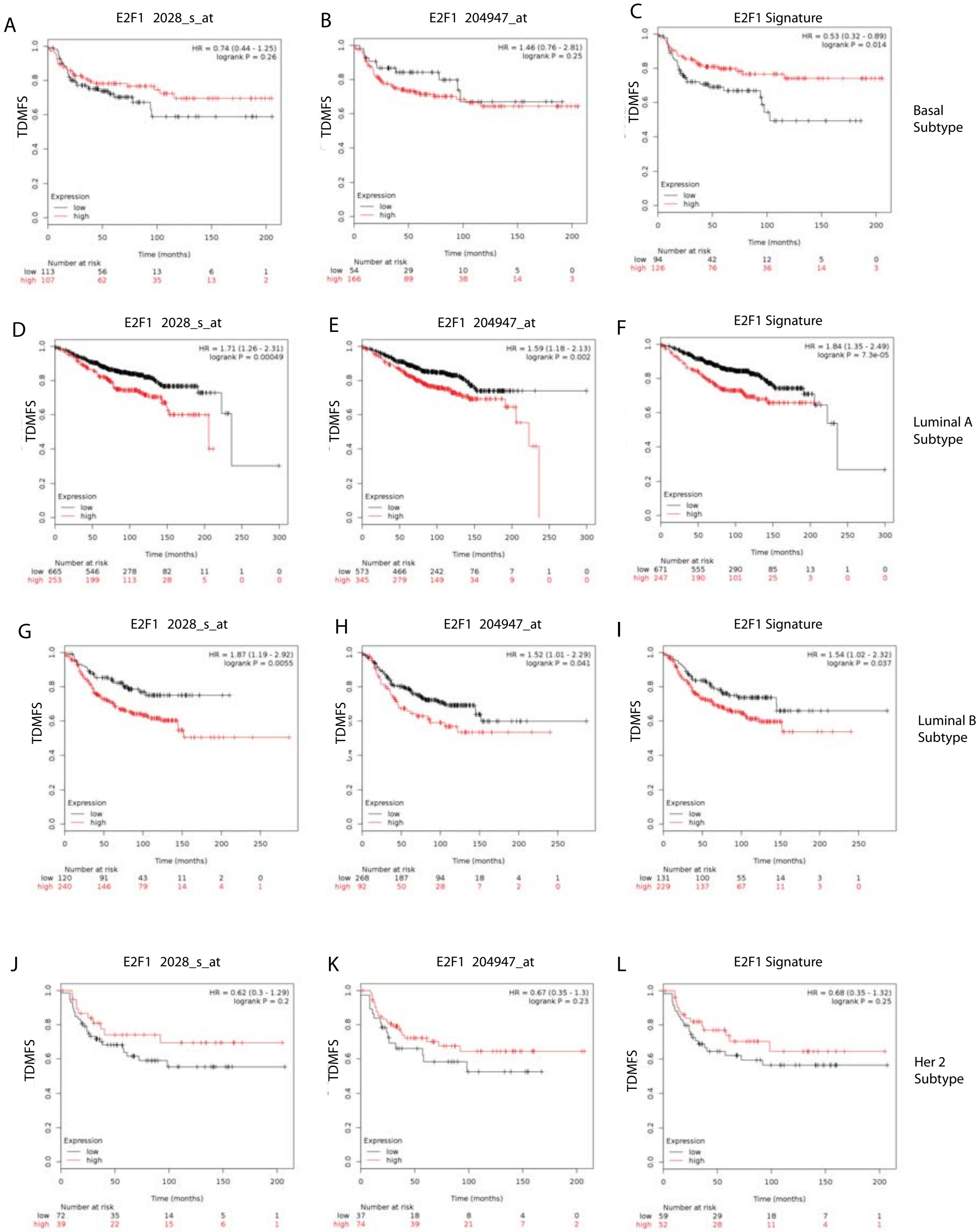
A
E2F1 2028_s_at
HR = 0.74 (0.44 - 1.25)
logrank P = 0.26
B
E2F1 204947_at
HR = 1.46 (0.76 - 2.81)
logrank P = 0.25
C
E2F1 Signature
HR = 0.53 (0.32 - 0.89)
logrank P = 0.014
Basal Subtype
D
E2F1 2028_s_at
HR = 1.71 (1.26 - 2.31)
logrank P = 0.00049
E
E2F1 204947_at
HR = 1.59 (1.18 - 2.13)
logrank P = 0.002
F
E2F1 Signature
HR = 1.84 (1.35 - 2.49)
logrank P = 7.3e-05
Luminal A Subtype
G
E2F1 2028_s_at
HR = 1.87 (1.19 - 2.92)
logrank P = 0.0055
H
E2F1 204947_at
HR = 1.52 (1.01 - 2.29)
logrank P = 0.041
I
E2F1 Signature
HR = 1.54 (1.02 - 2.32)
logrank P = 0.037
Luminal B Subtype
J
E2F1 2028_s_at
HR = 0.62 (0.3 - 1.29)
logrank P = 0.2
K
E2F1 204947_at
HR = 0.67 (0.35 - 1.3)
logrank P = 0.23
L
E2F1 Signature
HR = 0.68 (0.35 - 1.32)
logrank P = 0.25
Her 2 Subtype
TDMFS
Time (months)
Expression
low
high
Number at risk

Fig S3

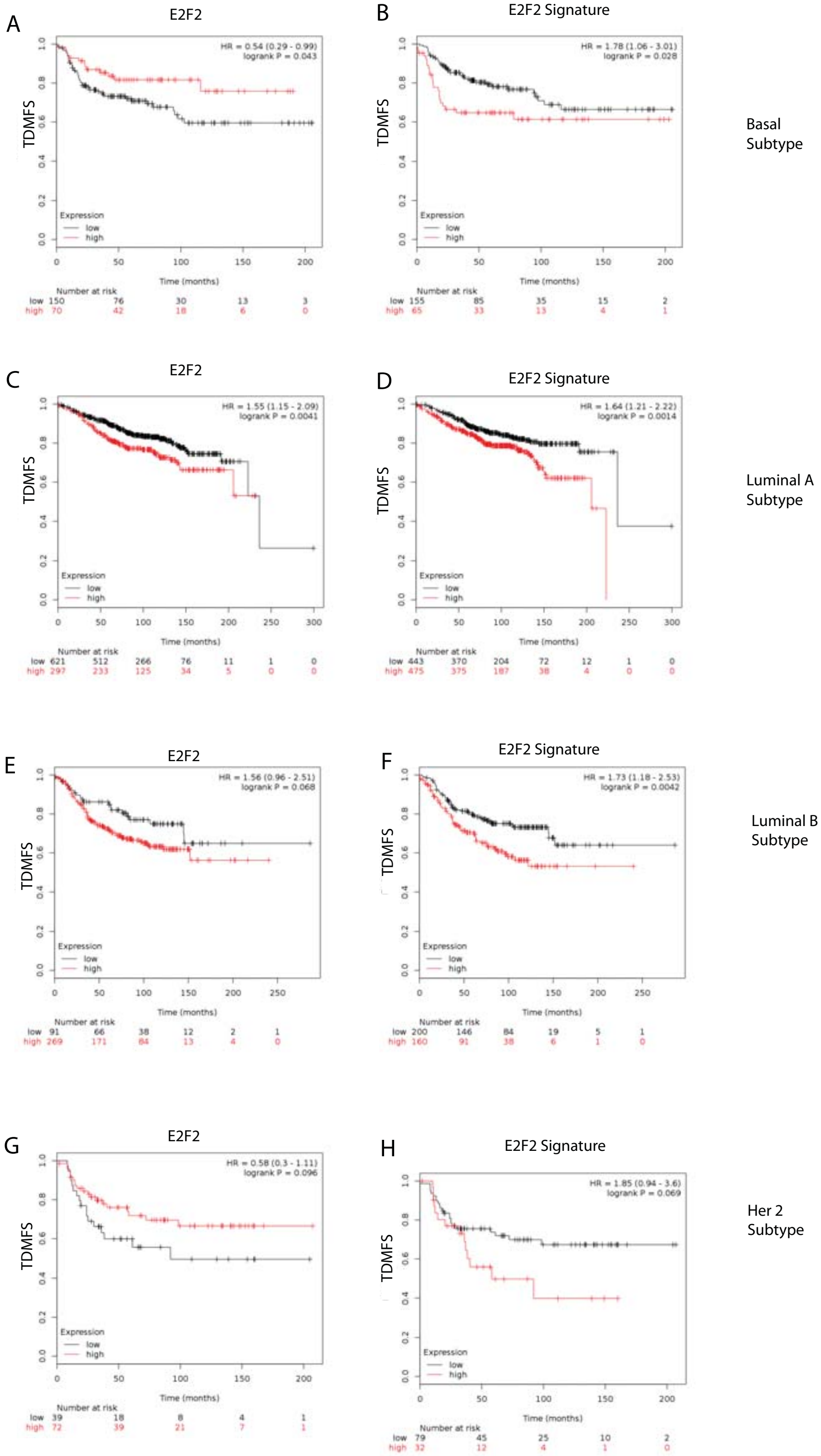
A
E2F2
HR = 0.54 (0.29 - 0.99)
logrank P = 0.043
TDMFS
Expression
low
high
Time (months)
Number at risk
low 150 76 30 13 3
high 70 42 18 6 0
B
E2F2 Signature
HR = 1.78 (1.06 - 3.01)
logrank P = 0.028
TDMFS
Expression
low
high
Time (months)
Number at risk
low 155 85 35 15 2
high 65 33 13 4 1
Basal
Subtype
C
E2F2
HR = 1.55 (1.15 - 2.09)
logrank P = 0.0041
TDMFS
Expression
low
high
Time (months)
Number at risk
low 621 512 266 76 11 1 0
high 297 233 125 34 5 0 0
D
E2F2 Signature
HR = 1.64 (1.21 - 2.22)
logrank P = 0.0014
TDMFS
Expression
low
high
Time (months)
Number at risk
low 443 370 204 72 12 1 0
high 475 375 187 38 4 0 0
Luminal A
Subtype
E
E2F2
HR = 1.56 (0.96 - 2.51)
logrank P = 0.068
TDMFS
Expression
low
high
Time (months)
Number at risk
low 91 66 38 12 2 1
high 269 171 84 13 4 0
F
E2F2 Signature
HR = 1.73 (1.18 - 2.53)
logrank P = 0.0042
TDMFS
Expression
low
high
Time (months)
Number at risk
low 200 146 84 19 5 1
high 160 91 38 6 1 0
Luminal B
Subtype
G
E2F2
HR = 0.58 (0.3 - 1.11)
logrank P = 0.096
TDMFS
Expression
low
high
Time (months)
Number at risk
low 39 18 8 4 1
high 72 39 21 7 1
H
E2F2 Signature
HR = 1.85 (0.94 - 3.6)
logrank P = 0.069
TDMFS
Expression
low
high
Time (months)
Number at risk
low 79 45 25 10 2
high 32 12 4 1 0
Her 2
Subtype

Fig S4

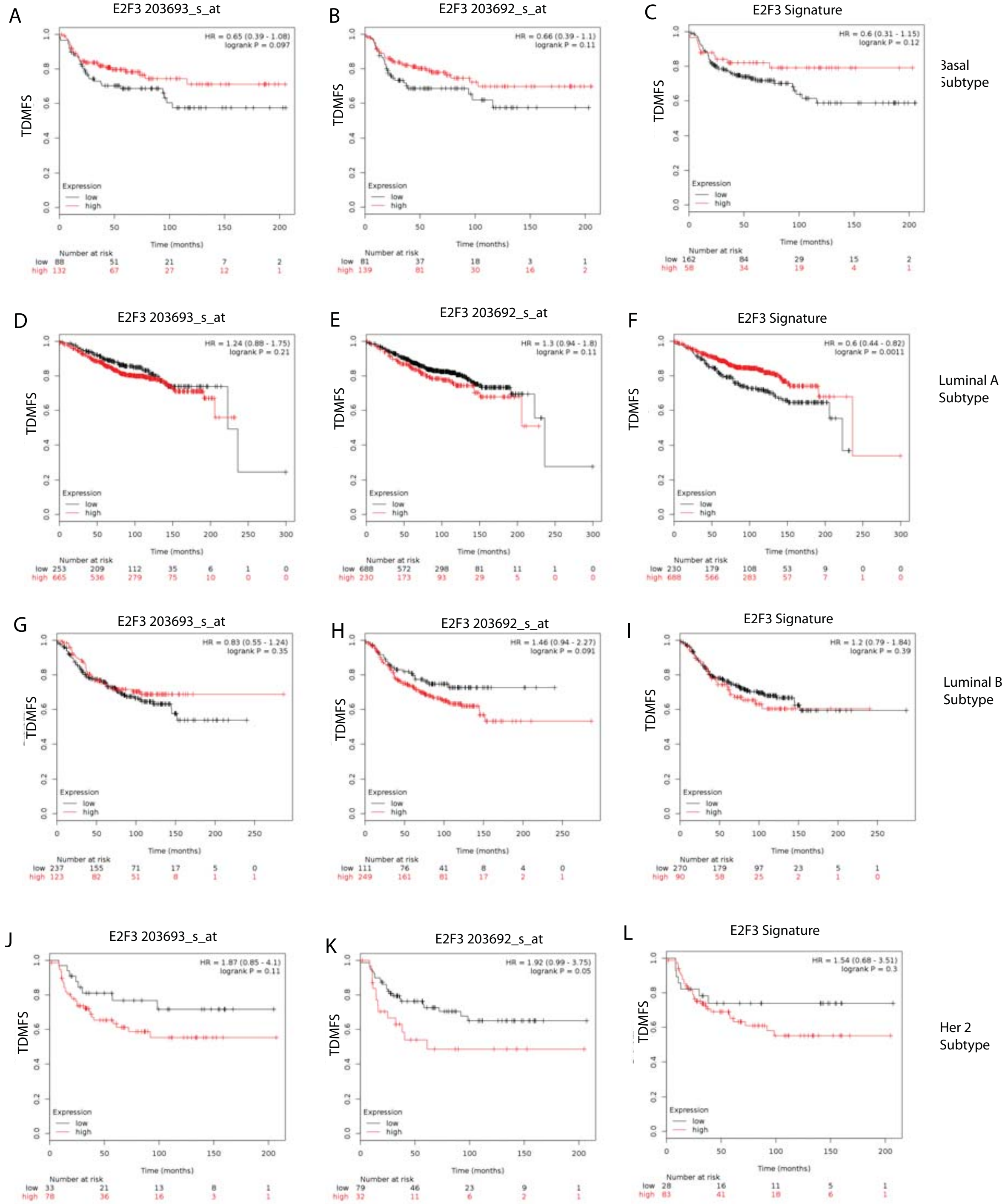
A
E2F3 203693_s_at
B
E2F3 203692_s_at
C
E2F3 Signature
Basal Subtype
D
E2F3 203693_s_at
E
E2F3 203692_s_at
F
E2F3 Signature
Luminal A Subtype
G
E2F3 203693_s_at
H
E2F3 203692_s_at
I
E2F3 Signature
Luminal B Subtype
J
E2F3 203693_s_at
K
E2F3 203692_s_at
L
E2F3 Signature
Her 2 Subtype
TDMFS
HR = 0.65 (0.39 - 1.08) logrank P = 0.097
HR = 0.66 (0.39 - 1.1) logrank P = 0.11
HR = 0.6 (0.31 - 1.15) logrank P = 0.12
HR = 1.24 (0.88 - 1.75) logrank P = 0.21
HR = 1.3 (0.94 - 1.8) logrank P = 0.11
HR = 0.6 (0.44 - 0.82) logrank P = 0.0011
HR = 0.83 (0.55 - 1.24) logrank P = 0.35
HR = 1.46 (0.94 - 2.27) logrank P = 0.091
HR = 1.2 (0.79 - 1.84) logrank P = 0.39
HR = 1.87 (0.85 - 4.1) logrank P = 0.11
HR = 1.92 (0.99 - 3.75) logrank P = 0.05
HR = 1.54 (0.68 - 3.51) logrank P = 0.3
Expression
low
high
Time (months)
Number at risk

Fig S5

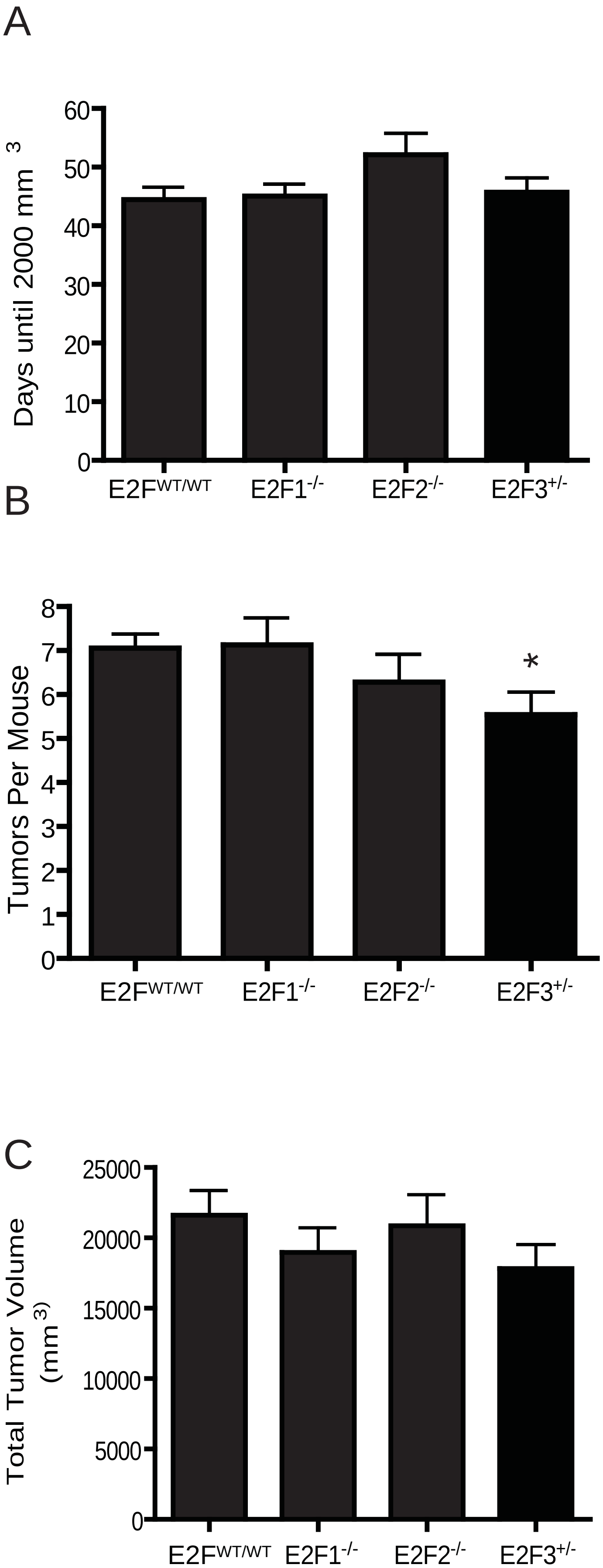
A
Days until 2000 mm 3
60
50
40
30
20
10
0
E2FWT/WT
E2F1-/-
E2F2-/-
E2F3+/-
B
Tumors Per Mouse
8
7
6
5
4
3
2
1
0
*
E2FWT/WT
E2F1-/-
E2F2-/-
E2F3+/-
C
Total Tumor Volume
(mm3)
25000
20000
15000
10000
5000
0
E2FWT/WT
E2F1-/-
E2F2-/-
E2F3+/-

Fig S6

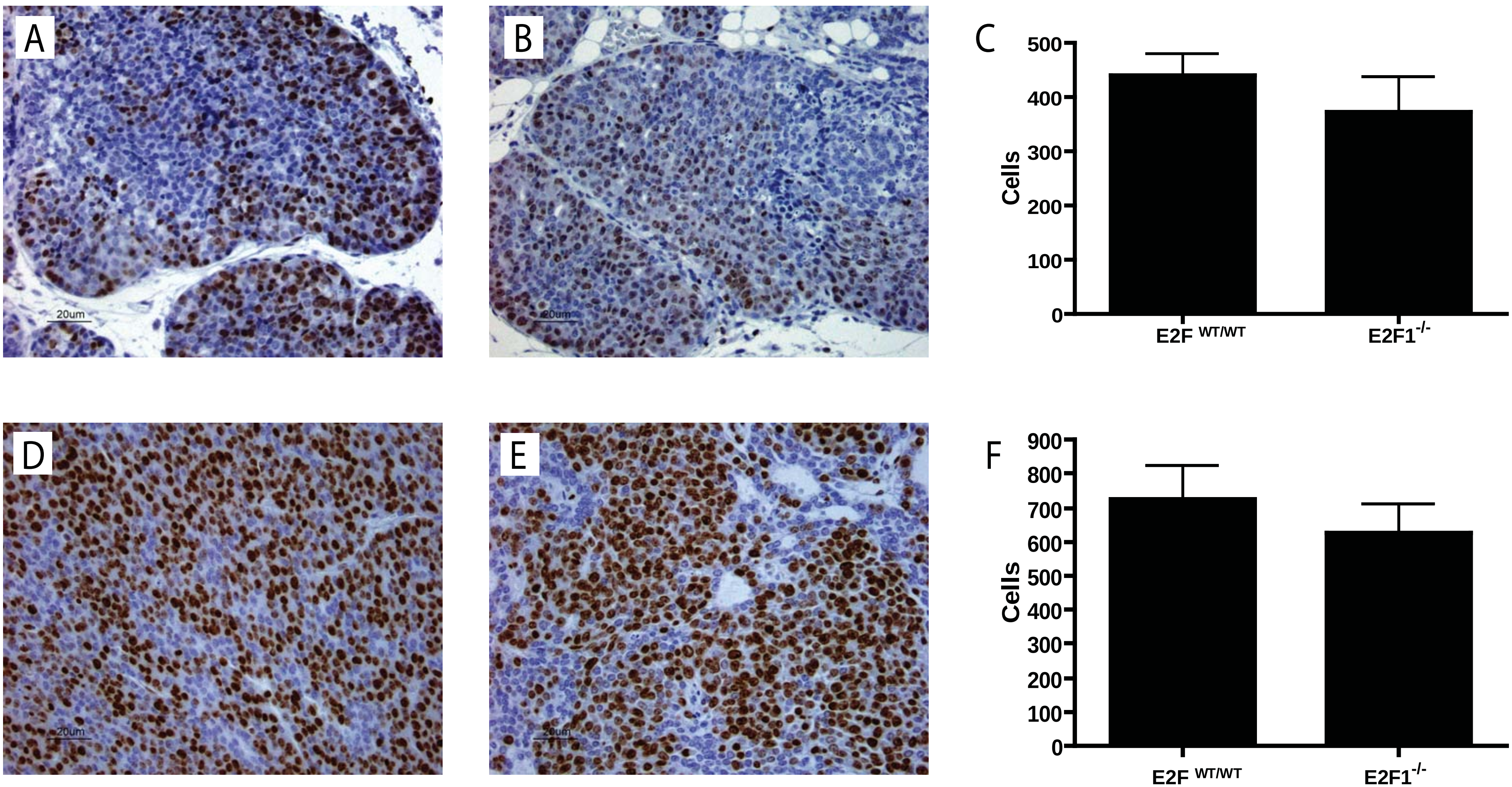
A
20um
B
20um
C
Cells
500
400
300
200
100
0
E2F WT/WT
E2F1-/-
D
20um
E
20um
F
Cells
900
800
700
600
500
400
300
200
100
0
E2F WT/WT
E2F1-/-

Fig S7

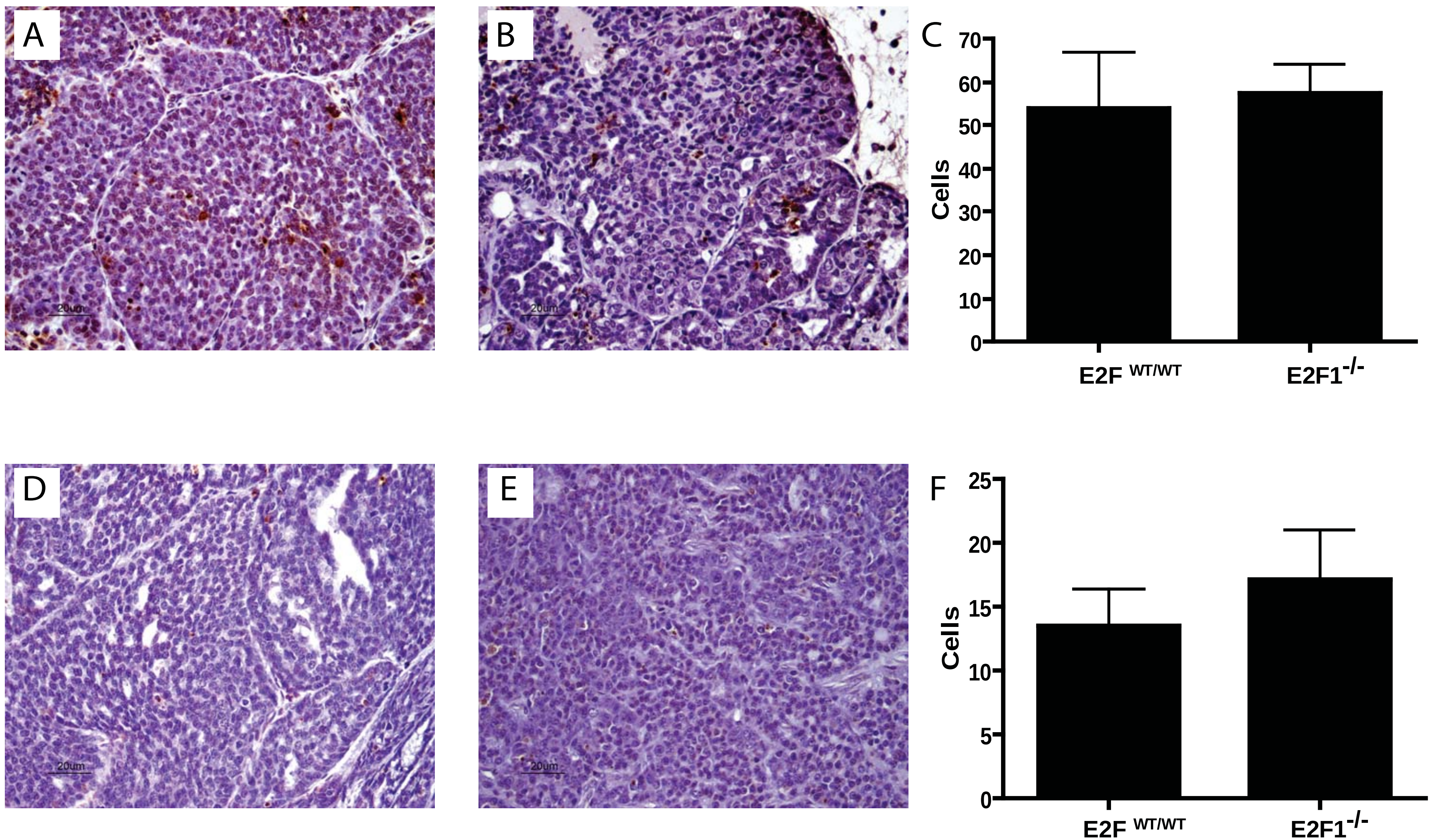
A
20um
B
20um
C
Cells
70
60
50
40
30
20
10
0
E2F WT/WT
E2F1-/-
D
20um
E
20um
F
Cells
25
20
15
10
5
0
E2F WT/WT
E2F1-/-

Fig S8

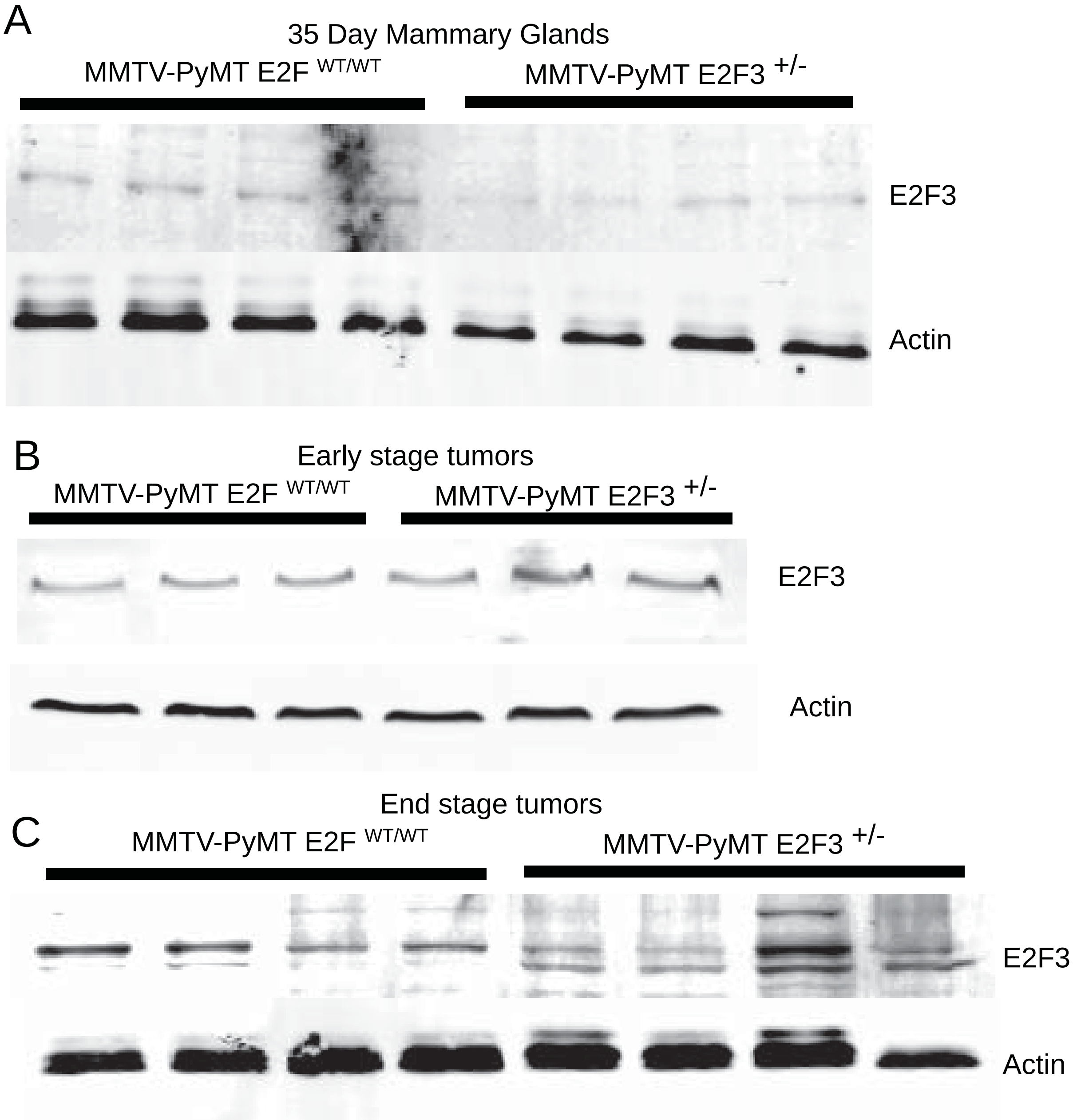
A
35 Day Mammary Glands
MMTV-PyMT E2F WT/WT
MMTV-PyMT E2F3 +/-
E2F3
Actin
B
Early stage tumors
MMTV-PyMT E2F WT/WT
MMTV-PyMT E2F3 +/-
E2F3
Actin
C
End stage tumors
MMTV-PyMT E2F WT/WT
MMTV-PyMT E2F3 +/-
E2F3
Actin

Fig S9

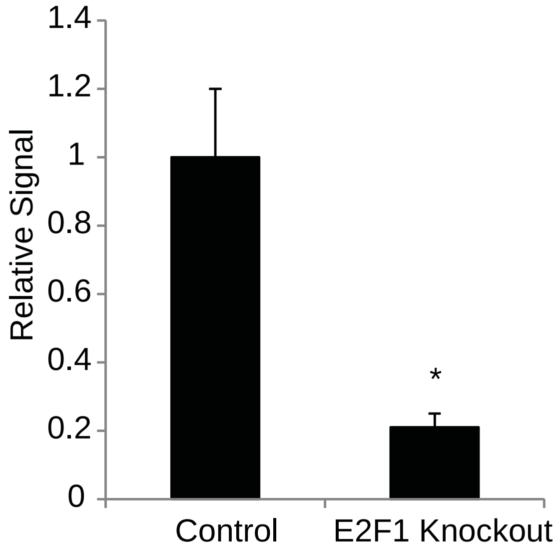

Fig S10

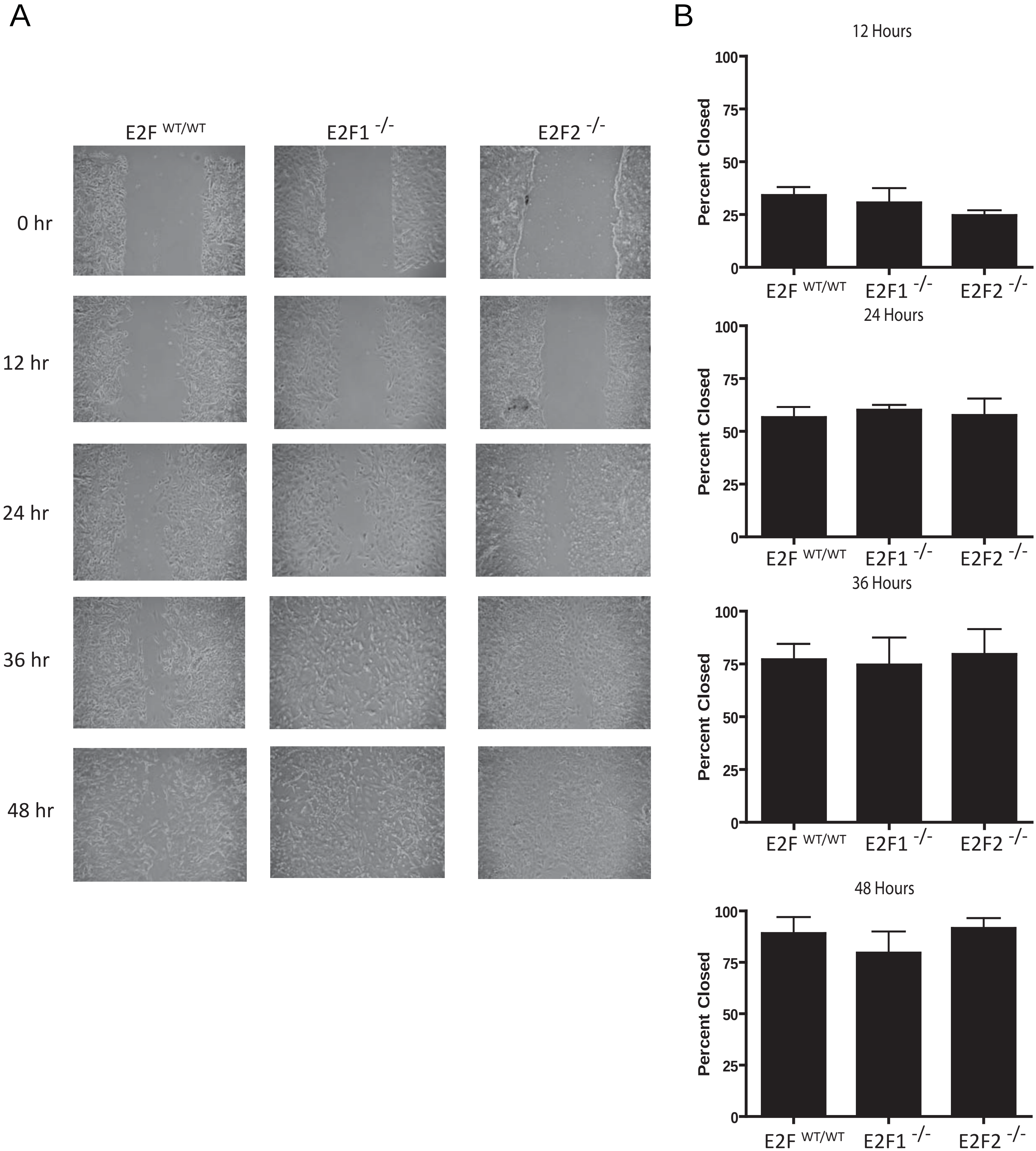
A
E2F WT/WT
E2F1 -/-
E2F2 -/-
0 hr
12 hr
24 hr
36 hr
48 hr
B
12 Hours
24 Hours
36 Hours
48 Hours
Percent Closed
0
25
50
75
100
E2F WT/WT
E2F1 -/-
E2F2 -/-

Fig S11

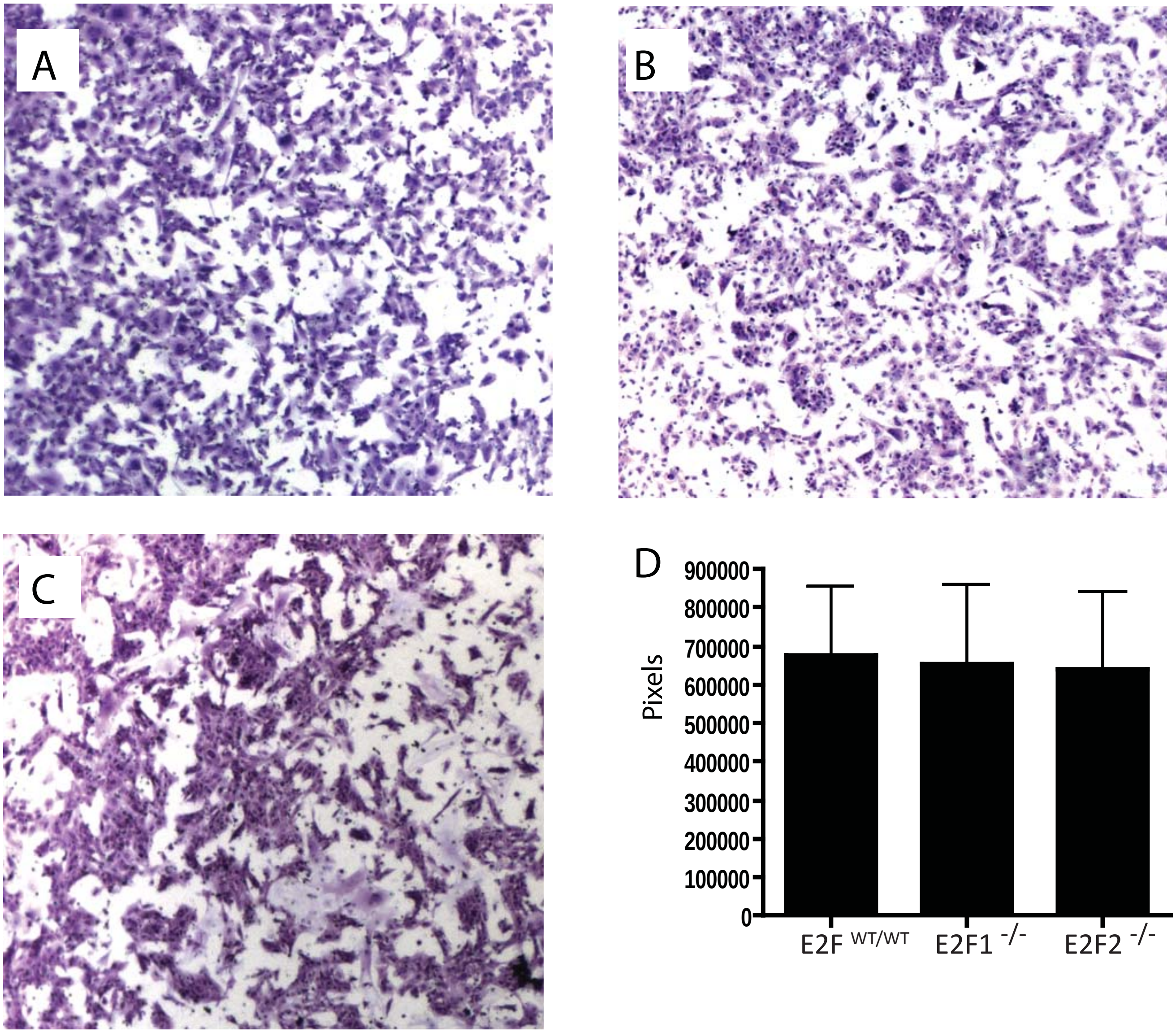
A
B
C
D
900000
800000
700000
600000
500000
400000
300000
200000
100000
0
Pixels
E2F WT/WT
E2F1 -/-
E2F2 -/-

Fig S12

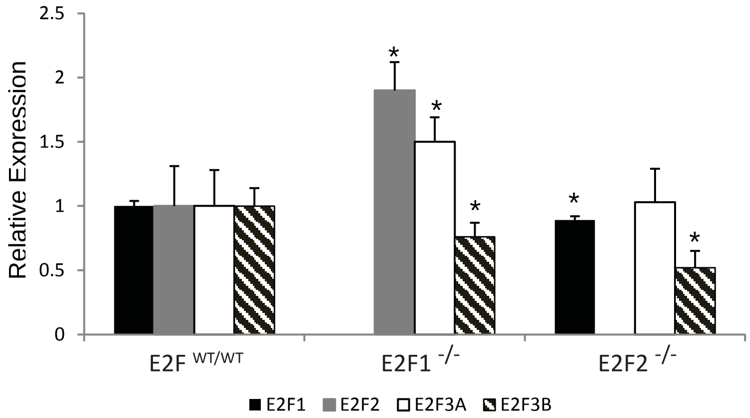

Relative Expression
2.5
2
1.5
1
0.5
0
*
E2F WT/WT
E2F1 -/-
E2F2 -/-
E2F1
E2F2
E2F3A
E2F3B

Fig S13

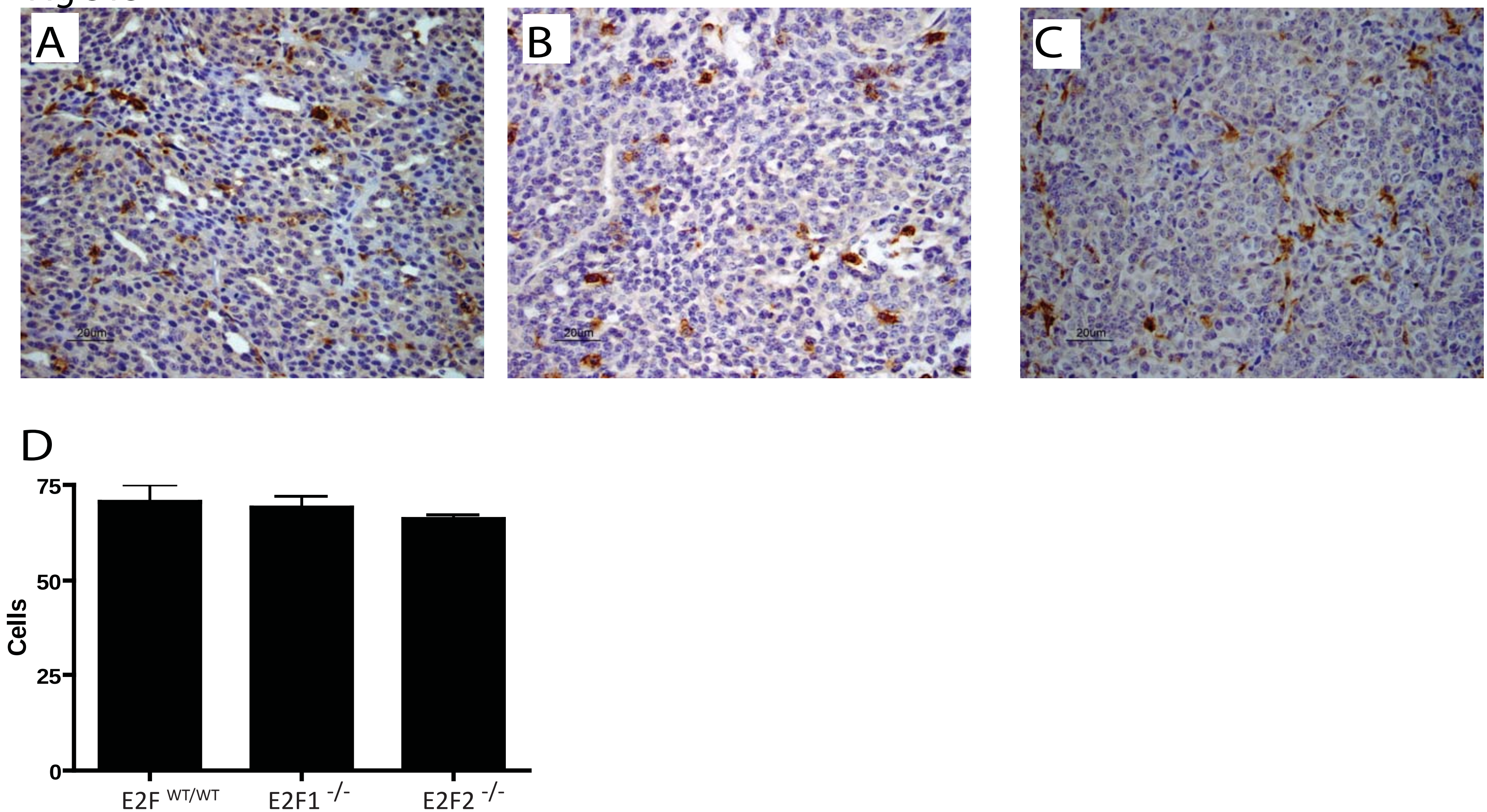

Fig S1- Association E2F signature genes with human breast cancer distant metastasis free survival times.

(A)Using the average expression of the upregulated genes in the E2F1 signature, a correlation ($p=0.00024$) with a shorter time to distant metastasis in human breast cancer patients ($n=1610$) was detected. (B) Using the average expression of the upregulated genes in the E2F2 signature, a correlation ($p=0.000037$) with a shorter time to distant metastasis in human breast cancer patients ($n=1610$) was detected. (C)Using the average expression of the upregulated genes in the E2F3 signature, a correlation ($p=0.0052$) with a longer time to distant metastasis in human breast cancer patients ($n=1610$) was detected. Patient stratification was conducted using the www.kmplot.com auto selection tool.

Fig S2- Association of E2F1 levels and signature genes distant metastasis free survival times within specific intrinsic subtypes of human breast cancer.

For each analysis using signature genes the average expression of the upregulated genes in the E2F1 signature were used during stratification. (A-C) The association of E2F1 levels and signature genes within the basal subtype of breast cancer are shown. (D-F) The association of E2F1 levels and signature genes with metastasis events in the luminal A subtype of breast cancer are shown($p=0.0049$ for 2028_s_at, $p=0.002$ for 204947_at, and $p=0.000073$ for the analysis using the signature genes). (G-I) The association of E2F1 levels and signature genes with metastasis events in the luminal B subtype of breast cancer are shown($p=0.0055$ for 2028_s_at, $p=0.041$ for 204947_at, and $p=0.037$ for the analysis using the signature genes). (J-L) The association of E2F1 levels and signature genes within the Her2 subtype of breast cancer are shown.

Fig S3- Association of E2F2 levels and signature genes distant metastasis free survival times within specific intrinsic subtypes of human breast cancer.

For each analysis using signature genes the average expression of the upregulated genes in the E2F2 signature were used during stratification. (A-B) The association of E2F2 levels and signature genes within the basal subtype of breast cancer are shown. While high levels of E2F2 are protective (p=0.043, high expression E2F2 signature genes predict faster onset of distant metastasis(p=0.028) (C-D) The association of E2F2 levels and signature genes with metastasis events in the luminal A subtype of breast cancer are shown(p=0.0041 for E2F2 levels, p=0.0014 for the analysis using the signature genes). (E-F) The association of E2F2 levels and signature genes with metastasis events in the luminal B subtype of breast cancer are shown(p=0.0042 for the analysis using the signature genes). (G-H) The association of E2F2 levels and signature genes within the Her2 subtype of breast cancer are shown.

Fig S4- Association of E2F3 levels and signature genes distant metastasis free survival times within specific intrinsic subtypes of human breast cancer.

For each analysis using signature genes the average expression of the upregulated genes in the E2F3 signature were used during stratification. (A-C) The association of E2F3 levels and signature genes within the basal subtype of breast cancer are shown. (D-F) The association of E2F3 levels and signature genes with metastasis events in the luminal A subtype of breast cancer are shown. (G-I) The association of E2F3 levels and signature genes with metastasis events in the luminal B subtype of breast cancer are shown. (J-L) The association of E2F3 levels and signature genes within the Her2 subtype of breast cancer are shown.

Fig S5- Loss of E2Fs does not affect tumor growth rate or tumor burden.

(A)The average tumor growth rate is depicted by the days until the primary tumor reaches 2,000mm^3 from initial palpation. At tumor endpoint, the number of tumors present on each mouse was counted. (B) The average number of tumors per mouse for each population of E2F$^{WT/WT}$ or mutant mice. (C) The average volume (mm^3) from the sum of each tumor present within a mouse. All error bars represent SEM. All comparisons were made between E2F wild type controls and E2F knockout mice using a T-Test.

Fig S6- E2F1 loss has no effect on KI67 staining in early or late staged tumors.

(A) Representative IHC staining for KI67 in early stage (diameter=6mm) E2F$^{WT/WT}$ tumors (n=5). (B) Representative IHC staining for KI67 in early stage (diameter=6mm) E2F1$^{-/-}$tumors (n=5).(C) Quantification of IHC results showing the average number of KI67 positive cells per field in E2F$^{WT/WT}$ and E2F1$^{-/-}$ early stage tumors. (D) Representative IHC staining for KI67 in end stage (diameter=20mm) E2F$^{WT/WT}$ tumors (n=5). (E) Representative IHC staining for KI67 in end stage (diameter=20mm) E2F1$^{-/-}$tumors (n=5). (F) Quantification of IHC results showing the average number of KI67 positive cells per field in E2F$^{WT/WT}$ and E2F1$^{-/-}$ end stage tumors.

Fig S7- E2F1 loss has no effect on TUNEL staining in early or late staged tumors.

(A) Representative IHC staining for TUNEL in early stage (diameter=6mm) E2F$^{WT/WT}$ tumors (n=5). (B) Representative IHC staining for TUNEL in early stage (diameter=6mm) E2F1$^{-/-}$ tumors (n=5).(C) Quantification of IHC results showing the average number of TUNEL positive cells per field in E2F$^{WT/WT}$ and E2F1$^{-/-}$ early stage tumors. (D) Representative IHC staining for TUNEL in end stage (diameter=20mm) E2F$^{WT/WT}$ tumors (n=5). (E) Representative IHC staining for TUNEL in end stage (diameter=20mm) E2F1$^{-/-}$tumors (n=5). (F) Quantification of IHC results showing the average number of TUNEL positive cells per field in $E2F^{WT/WT}$ and $E2F1^{-/-}$ end stage tumors.

Fig S8- Western blot analysis shows E2F3 protein levels at various stages of MMTV-PyMT tumor development.

(A) A comparison of E2F3 protein levels in 35 day old mammary glands in E2F WT (n=4) and $E2F3^{+/-}$ (n=4) glands. (B) A comparison of E2F3 protein levels in early stage (diameter= 6mm) tumors from $E2F^{WT/WT}$ (n=3) and $E2F3^{+/-}$ (n=3) mice. (C) A comparison of E2F3 protein levels in end stage (diameter= 20mm) tumors from $E2F^{WT/WT}$ (n=4) and $E2F3^{+/-}$ (n=4) mice.

Fig S9- Loss of E2Fs reduces transgenic signal for circulating tumor cells.

A comparison of qRT-PCR signal for expression of the transgene circulating tumor cell marker in transgenic control mice and E2F1 knockoout mice reveals that loss of E2F1 significantly ($p<.0001$) reduces circulating tumor cells.

Fig S10- Wound healing assay shows migratory ability of tumor derived cells from $E2F^{WT/WT}$, $E2F1^{-/-}$, and $E2F2^{-/-}$ mice.

(A) Representative pictures of wound closure at indicated time points for $E2F^{WT/WT}$, $E2F1^{-/-}$, and $E2F2^{-/-}$ tumor cells. (B) Quantification of wound closure at indicated time points for $E2F^{WT/WT}$, $E2F1^{-/-}$, and $E2F2^{-/-}$ tumor cells.

Fig S11- Transwell invasion assay shows migratory ability of tumor derived cells from $E2F^{WT/WT}$, $E2F1^{-/-}$, and $E2F2^{-/-}$ mice.

(A) Representative picture for $E2F^{WT/WT}$ tumor cell migration in the transwell invasion assay. (B) Representative picture for $E2F1^{-/-}$ tumor cell migration in the transwell invasion assay. (C)

Representative picture for $E2F2^{-/-}$ tumor cell migration in the transwell invasion assay. (D) Quantification of transwell invasion assay for $E2F^{WT/WT}$, $E2F1^{-/-}$ and $E2F2^{-/-}$ tumor cells.

Fig S12- Relative expression of E2F1, E2F2, E2F3A, and E2F3B in MMTV-PyMT transplanted tumors.

$E2F1^{-/-}$ tumors (n=4) had a significant increase in E2F2 (p=0.0032)and E2F3A (p=0.0254) expression with a significant decrease in E2F3B (p=0.0358). Similar to the spontaneous tumors, $E2F2^{-/-}$ transplanted tumors had a significant decrease in E2F1 expression (p=0.0046) and a significant downregulation (p=0.0024) of E2F3B.

Fig S13- E2F loss has no effect on F4/80 staining in end stage tumors.

(A) Representative IHC staining for F4/80 in end stage (diameter=20mm) $E2F^{WT/WT}$ tumors (n=5). (B) Representative IHC staining for F4/80 in end stage (diameter=20mm) $E2F1^{-/-}$ tumors (n=5).(C) Representative IHC staining for F4/80 in end stage (diameter=20mm) $E2F2^{-/-}$ tumors (n=5) (D) Quantification of IHC results showing the average number of F4/80 positive cells per field across the various indicated genotypes.